Hindawi
Advances in Materials Science and Engineering
Volume 2023, Article ID 9840714, 1 page
https://doi.org/10.1155/2023/9840714

Retraction

Retracted: Experimental Analysis and Optimization of Tribological Properties of Self-Lubricating Aluminum Hybrid Nanocomposites Using the Taguchi Approach

Advances in Materials Science and Engineering

Received 26 December 2023; Accepted 26 December 2023; Published 29 December 2023

This article has been retracted by Hindawi, as publisher, following an investigation undertaken by the publisher [1]. This investigation has uncovered evidence of systematic manipulation of the publication and peer-review process. We cannot, therefore, vouch for the reliability or integrity of this article.

Please note that this notice is intended solely to alert readers that the peer-review process of this article has been compromised.

Wiley and Hindawi regret that the usual quality checks did not identify these issues before publication and have since put additional measures in place to safeguard research integrity.

We wish to credit our Research Integrity and Research Publishing teams and anonymous and named external researchers and research integrity experts for contributing to this investigation.

The corresponding author, as the representative of all authors, has been given the opportunity to register their agreement or disagreement to this retraction. We have kept a record of any response received.

References

[1] V. K. Selvaraj, S. Jeyanthi, R. Thiyagarajan et al., "Experimental Analysis and Optimization of Tribological Properties of Self-Lubricating Aluminum Hybrid Nanocomposites Using the Taguchi Approach," *Advances in Materials Science and Engineering*, vol. 2022, Article ID 4511140, 13 pages, 2022.

Hindawi
Advances in Materials Science and Engineering
Volume 2022, Article ID 4511140, 13 pages
https://doi.org/10.1155/2022/4511140

Research Article

Experimental Analysis and Optimization of Tribological Properties of Self-Lubricating Aluminum Hybrid Nanocomposites Using the Taguchi Approach

Vinoth Kumar Selvaraj,[1] S. Jeyanthi,[1] Raja Thiyagarajan,[1] M. Senthil Kumar,[1] L. Yuvaraj,[2] P. Ravindran,[3] D. M. Niveditha,[1] and Yigezu Bantirga Gebremichael [4]

[1]*School of Mechanical Engineering, Vellore Institute of Technology, Chennai 600127, Tamilnadu, India*
[2]*Department of Automobile Engineering, Acharya Institute of Technology, Bangalore 560107, Karnataka, India*
[3]*Department of Mechanical Engineering, St. Mother Theresa Engineering College, Vagaikulam, Thoothukudi, Tamilnadu, India*
[4]*School of Mechanical and Chemical Engineering, Kombolcha Institute of Technology, Wollo University, Kombolcha, Ethiopia*

Correspondence should be addressed to Yigezu Bantirga Gebremichael; yigezu@kiot.edu.et

Received 6 July 2022; Accepted 8 September 2022; Published 4 October 2022

Academic Editor: K. Raja

In recent times, tribological properties are gaining and grabbing great attention in metal matrix composites. They can provide significant benefits such as a lower coefficient of friction, wear resistance, high strength, and stiffness. Considering all these parameters, this research article mainly focuses on developing an aluminum hybrid nanocomposite material fabricated by powder metallurgy. Then, the results were examined using a pin-on-disk apparatus. Further optimization techniques such as the Taguchi approach under Design of Experiments have been adopted to obtain a minimal outcome of various assumed parameters such as A. percentage weight fraction of graphite content (Gr), B. the sliding distance, C. the sliding speed, and D. the stress applied. In addition, we have chosen parameters such as friction and wear loss for optimizing the outcome, including the main effect plots for the S-N ratio and the Analysis of Variance (ANOVA) approach. Based on the experimental results, we have noticed that friction and wear loss coefficient increase with increased applied load and sliding distance. Also, it was noted that there was a slight decrease in the coefficient of friction and wear loss when an increment was made in the graphite content, respectively. It was perceived that the sample containing 10% of graphite (Gr) could create a self-lubricating effect that significantly reduced wear loss and the coefficient of friction. Finally, by considering all these achieved results, aluminum nanocomposites can be employed in automobile, defense, and aerospace applications as they can reduce the weight of the components with improved wear behavior and more thermal stability.

1. Introduction

Recent research has reported that metal matrix composites with aluminum have exhibited low density and the ability to strengthen the material by precipitation, corrosion resistivity, thermal stability, and high electrical conductivity for potential tribological applications in the automotive and aerospace industries [1, 2]. It was found that inserting ceramic particles such as graphite, silicon carbide, aluminum oxide, and titanium carbide improved the noticeable tribological and mechanical properties of AMMCs [3–7]. Practical aluminum-based exhibits not only have high mechanical and wear properties but are capable of achieving self-lubricating properties.

Because the metal matrix is one of the traditional composites with various nanofillers, aluminum matrix alloys can significantly improve both mechanical and mechanical self-lubrication properties [8, 9]. Aluminum with silicon carbide composites reinforced with graphite nanofillers was used to create a combination of Al-SiC-Gr hybrid composites [10]. Furthermore, due to their exceptional features, the market for hybrid composites has grown dramatically in

the last five years. Furthermore, it was found that the creation of nano-crystalline hybrid AMMCs has a much higher strength than microcrystalline composites [11]. Numerous reports and experimental studies have been conducted on aluminum nanoparticles' dry condition wear behavior. It has been reported that the combination of aluminum and silicon carbide reduces the coefficient of friction; the addition of 10% silicon carbide and 6% graphite increased the bulk mechanical characteristics [12]. It has resulted from the combined action of an aluminum matrix combined with graphite and ceramics, resulting in noticeable good wear characteristics [13]. The influence of silicon carbide content on Al6061 was studied using silicon carbide and graphite hybrid composite processing, compact behavior, and properties using in-situ powder metallurgy (IPM) technology [14]. Most of the work was focused on and carried out on experimental work. Also, few mathematical models were based on factorial or Taguchi approaches [15, 16].

This has resulted from using liquid metallurgy to investigate the effect of sliding speed on the dry condition of wear behavior of hybrid metal matrix composites. Furthermore, many investigations were conducted using silicon carbide/Gr aluminum composite, including squeeze casting and stir-casting [17]. The homogenous reinforcing distribution is a benefit of powder metallurgy. The structural, mechanical, and high wear resistance properties are all improved by this homogenous distribution. According to literature sources, the number of investigations into the tribological behavior of hybrid composites is quite restricted. The majority of the published research studies, on the other hand, concentrated on the consequences and effects of several constraints on sliding wear and coefficient of friction and their behavior towards hybrid composites [18]. From the extensive literature survey, very minimal experimental work was carried out in the study, mainly focused on characteristics and parameters that influence the tribological behavior of nanohybrid composites. Most of the reported works were targeted at micron-size particle-reinforced aluminum composites [19, 20]. The novelty of this present investigation is to explore the optimized wear behavior of the nano-SiC and Gr-reinforced aluminum matrix composites using Taguchi design. The automobile wear components are the targeted applications for the developed aluminum matrix composites.

The primary objective of this research article is to utilize powder metallurgy to fabricate a nanohybrid aluminum metal matrix composite and practice the Taguchi approach under Design of Experiments to analyze the optimal outcomes of the coefficient of friction and wear loss [21]. By expanding the usage of fractional factorial design to include orthogonal arrays, Taguchi's experimental design, response surface methodology, and others can further simplify the trials [22–26]. Based on the results, this method offers a quick and flexible way to improve the outcome's performance, cost-effectiveness, and quality. Also, the current research attempts to investigate and optimize various parameters such as graphite reinforcement, the load applied, sliding distance, and sliding speed on the wear behavior of aluminum hybrid nanocomposites. Apart from the factors mentioned earlier, Taguchi's experimental approach and ANOVA are adopted to evaluate the obtained results and determine the effect of the percentage of various components on the fabricated composite material. At the same time, microstructure of the fractured surfaces and analysis of worn surfaces of the pin was studied using SEM. It is characterized to understand the better wear mechanism and analyze the topography of the fractured surfaces.

Table 1: Specifications of nano-fillers used in the base material.

Nanofillers	Density (g/cm^3)	Melting point	Grain size (nm)
Silicon carbide	3.22	2730	100
Graphite	2.26	3600	40–50

2. Materials and Methodology

2.1. Materials Required for the Fabrication of Aluminum Hybrid Nanocomposites. The nanocomposites were synthesized using the powder metallurgy approach. In this present research work, aluminum alloy 2024 is used as the base material, and the chemical composition of aluminum matrix AA 2024 is (Cu-4%, Mg-1.7 to 1.8%, Fe-0.5%, Mn-0.23 to 0.25%, Si-0.3 to 0.5%, Cr-0.25%, and Zn-0.2%, and balance is aluminum). The main reason for choosing aluminum alloy as a matrix material is that it is considered excellent for corrosion resistance, strength, and damage tolerance at high and low temperatures. In addition to these, four different hybrid nanocomposites were created, including AA2024, AA2024 with 5% silicon carbide, AA2024 with 5% SiC and 5% Gr, and AA2024 with 5% SiC and 10% Gr, respectively. Specifications for silicon carbide and graphite are listed in Table 1. At the same time, the mechanical properties of the fabricated hybrid nanocomposites are listed in Table 2.

2.2. Preparation of Hybrid Nanocomposites. A mixture of Al 2024, SiC, and Gr powders were ground in a planetary ball mill to create a hybrid Al nanocomposite. All four different types of powder mixes were put through a high-energy planetary ball milling process using vials and tungsten balls. The mechanical alloying procedure was carried out at 300 rpm in a toluene medium to prevent oxidation or powder adhering to the vial wall. The powder was ground for up to 2 h using tungsten balls with a 10 mm diameter and a 10:1 ball-to-powder weight ratio. It is manually applied earlier to each trial. The literature review reported that the combination of powders was hard-pressed in a uniaxial press where pressure is maintained at 700 MPa for generating green compacts. It was also reported that sintering of the compacts was conducted for 60 min at a controlled temperature of 530°C [27]. In addition, all of the sintered composites were subjected to a solution treatment in a furnace at a temperature of 540°C for roughly 120 min, followed by a 72-hour water quenching process. Wear specimens are fabricated, ensuring that the diameter is 8 mm with a height of 30 mm. Meanwhile, the specimen edges are polished with various grades of emery paper. According to

Table 2: Mechanical properties of the fabricated aluminum with silicon carbide and graphite nanocomposites.

S. no.	Chemical mixture (wt. %)	Experimental density (g/cm^3)	Predicted density (g/cm^3)	Porosity (%)
1	Aluminum alloy (AA) 2024	2.857	2.912	1.888
2	AA2024/5% silicon carbide nanocomposite	2.902	2.941	1.326
3	AA2024/5% silicon carbide/5% graphite hybrid nanocomposite	2.864	2.924	2.051
4	AA2024/5% silicon carbide/10% graphite hybrid nanocomposite	2.841	2.908	2.303

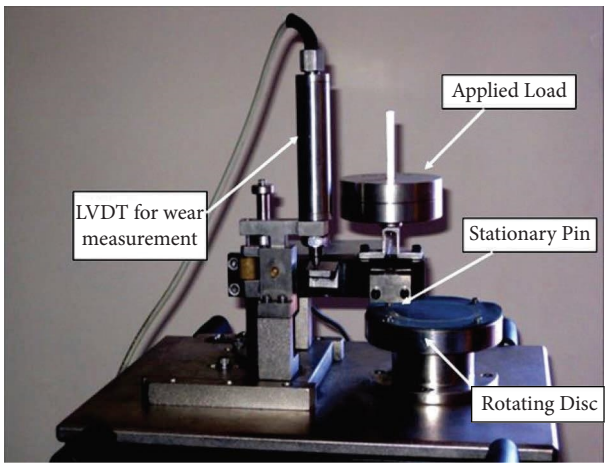

Figure 1: Components of the pin-on-disk test apparatus (Ducom, model no: ED-201).

Archimedes' principle, the actual density of the fabricated samples was measured using a high-accuracy weighing balance with a reading of 0.0001 mg. Besides, porosity is also determined by comparing the theoretical and actual density obtained from each sample.

2.3. Wear Test. The sliding wear characteristics were carried out using pin-on-disc equipment from Ducom, model No. 201, according to the ASTM G99-05 standard. EN31 steel was used for the counter disc, as shown in Figure 1. Before experimenting, all the pins and disc surfaces on the equipment were thoroughly cleaned with acetone. The tests were performed with loads ranging from 10 to 20 N. Also, sliding distances ranged from 500 to 2500 m with speeds of 1-2 m/s. After each trial, organic solvents such as acetone were used to clean the specimens and the counter face disc, which helped eliminate residues and impurities. The weight of the pins was evaluated before and after testing to determine the total wear loss. After six repetitions, the results of each test were noted and averaged at the end.

2.4. Sequential Steps to Perform Design of Experiments. In this research work, the experiment follows a three-level design based on the Design of Experiments (DOE) method. Factorial, Taguchi, RSM, and mixture are some of the different DOE techniques. A sophisticated design of experiments' tool is included in this Taguchi approach, which provides smart, efficient, high-quality systems for determining optimal parameter yields. Compared to the traditional experimental study method, this strategy significantly reduces the number of trial runs of experiments needed to design the response functions. According to conventional experimentation, it is also impossible to analyze all components and determine their separate impacts in a single experiment. The Taguchi technique has been adopted to overcome these drawbacks by considering all these factors. This Taguchi technique has been developed exclusively for minimizing processes that can optimize and find the best combinations of elements for specific outcomes. Each variety of trials was repeated or performed twice to achieve more optimized results. The signal-to-noise ratio (S/N) is calculated from the experimental data, and graphs are plotted accordingly. Various S/N ratios are possible depending on the type of experiments carried out. The S/N ratios are divided into three categories. They are smaller, considered the better one, whereas nominal is deemed the best ratio, respectively. For the minimal values of the coefficient of friction and wear loss, better characteristics are achieved in the S/N balance. The S/N ratio is considered using a logarithmic transformation of the loss function as represented in the following equation:

$$\frac{S}{N} = 10\mathrm{Log}\frac{1}{n}\left(\sum y^2\right), \tag{1}$$

where n = no. of observations and y = observed data.

From Table 3, we can identify the three levels for the four process parameters as (factors), which include (1) the weight percentage of graphite, (2) the applied load, (3) sliding distance, and (4) sliding speed. Table 4 represents a conventional Taguchi experimental plan with notation L_{27} (3^{13}). Table 5 describes the various conditions under which the trials were conducted. Minitab user manual software was used to create the mean-response plots, and ANOVA analysis was adopted to determine the % of influence in testing constraints [28].

3. Results and Discussions

3.1. Physical Measurements. According to Archimedes's principle, the physical measurement (density) of newly produced aluminum-based nanocomposites increased and reduced negligibly with the insertion of silicon carbide and graphite nanosize fillers into the AA 2024 as matrix material. The results also demonstrated that the experimental and predicted values were very similar. Figure 2 displays the density of hybrid nanocomposites as a function of grain content. This suggests that the experimental methods

Table 3: Input variables and levels for nanocomposites.

Input variables	Units	Level (I)	Level (II)	Level (III)
A: Graphite nanofillers	Wt. %	0	5	10
B: Applied load	N	10	15	20
C: Sliding distance	m	500	1500	2500
D: Sliding speed	m/s	1	1.5	2

Table 4: Orthogonal array L_{27} (3^{13}) of the Taguchi approach.

L_{27} (3^{13})	1	2	3	4	5	6	7	8	9	10	11	12	13
1	1	1	1	1	1	1	1	1	1	1	1	1	1
2	1	1	1	1	2	2	2	2	2	2	2	2	2
3	1	1	1	1	3	3	3	3	3	3	3	3	3
4	1	2	2	2	1	1	1	2	2	2	3	3	3
5	1	2	2	2	2	2	2	3	3	3	1	1	1
6	1	2	2	2	3	3	3	1	1	1	2	2	2
7	1	3	3	3	1	1	1	3	3	3	2	2	2
8	1	3	3	3	2	2	2	1	1	1	3	3	3
9	1	3	3	3	3	3	3	2	2	2	1	1	1
10	2	1	2	3	1	2	3	1	2	3	1	2	3
11	2	1	2	3	2	3	1	2	3	1	2	3	1
12	2	1	2	3	3	1	2	3	1	2	3	1	2
13	2	2	3	1	1	2	3	2	3	1	3	1	2
14	2	2	3	1	2	3	1	3	1	2	1	2	3
15	2	2	3	1	3	1	2	1	2	3	2	3	1
16	2	3	1	2	1	2	3	3	2	1	2	3	1
17	2	3	1	2	2	3	1	1	2	3	3	1	2
18	2	3	1	2	3	1	2	2	3	1	1	2	3
19	3	1	3	2	1	3	2	1	3	2	1	3	2
20	3	1	3	2	2	1	3	2	1	3	2	1	3
21	3	1	3	2	3	2	1	3	2	1	3	2	1
22	3	2	1	3	1	3	2	2	1	3	3	2	1
23	3	2	1	3	2	1	3	3	2	1	1	3	2
24	3	2	1	3	3	2	1	1	3	2	2	1	3
25	3	3	2	1	1	3	2	3	2	1	2	1	3
26	3	3	2	1	2	1	3	1	3	2	3	2	1
27	3	3	2	1	3	2	1	2	1	3	1	3	2

utilized in this study can develop near-dense materials. The experimental and predicted densities obtained from each sample were used to calculate the porosity of the materials. The lowest porosity samples (1.326 percent) were obtained, indicating that near-dense materials were received and that the alloying ingredient and reinforcement were successfully absorbed into the matrix. Figure 3 shows that as the weight percentage of graphite fillers increased, the porosity of the composites deteriorated.

3.2. Plan of Experiments. The orthogonal array is purely anticipated and based on the elementary limits of the degree of freedom, which is meant to be larger or equal to the number of parameters that are considered in wear accordingly, according to research and literature reviews on the orthogonal array [29]. It represents various factors and levels and their importance. The experiment comprises 27 experiments (one for each row of the L_{27} orthogonal array), which involve parameters allocated to each column. To perform an orthogonal array for our experiment, L27 was chosen. It contains 27 rows, 13 columns, and four wear parameters, namely (i) graphite (Gr) nanofillers, (ii) applied load, (iii) sliding distance, and (iv) sliding speed. In addition to these, the second column was labeled as graphite (Gr) reinforcement (A), the third column as load (B), the fourth as sliding distance (C), the fifth as sliding speed (D), and the remaining columns were labeled as interactions. Further, the trials were conducted utilizing the orthogonal array with varying degrees of freedom in each row. Finally, an Analysis of Variance was used to compare the results obtained from the wear test.

3.3. Analysis of Variance and Their Respective Effects over Factors. It is practical to understand the impact of various factors on the input parameters of graphite wt. % as reinforcement fillers, applied load, sliding distance, and sliding speed and their respective relations to the model analysis of the variance table to find the order of significance. Initially, a survey was conducted with a 95 percent level of significance. The results evaluated from the analysis of variance of hybrid

Table 5: Experimental design using L_{27} (3^{13}) orthogonal array.

(2^{13}) L_{27}	A	B	C	D	Wear loss (g)	Signal-to-noise ratio (dB)	Coefficient of friction	Signal-to-noise ratio (dB)
1	0	10	500	1.0	0.0035	49.118	0.149	17.289
2	0	10	1500	1.5	0.0106	38.493	0.162	16.171
3	0	10	2500	2.0	0.0203	33.850	0.177	15.801
4	0	15	500	1.5	0.0069	43.223	0.189	15.353
5	0	15	1500	2.0	0.0164	33.703	0.201	14.712
6	0	15	2500	1.0	0.0268	31.437	0.157	16.782
7	0	20	500	2.0	0.0082	41.723	0.214	14.322
8	0	20	1500	1.0	0.0159	36.756	0.187	15.366
9	0	20	2500	1.5	0.0351	29.093	0.199	14.921
10	5	10	500	1.5	0.0039	48.178	0.157	17.086
11	5	10	1500	2.0	0.0091	40.819	0.166	16.459
12	5	10	2500	1.0	0.0147	36.653	0.140	17.921
13	5	15	500	2.0	0.0041	47.744	0.155	16.359
14	5	15	1500	1.0	0.0101	39.913	0.149	17.623
15	5	15	2500	1.5	0.0230	32.765	0.151	17.292
16	5	20	500	1.0	0.0058	44.731	0.195	15.091
17	5	20	1500	1.5	0.0161	35.863	0.208	14.358
18	5	20	2500	2.0	0.0312	30.116	0.211	14.257
19	10	10	500	2.0	0.0027	51.372	0.169	16.346
20	10	10	1500	1.0	0.0059	44.583	0.161	16.157
21	10	10	2500	1.5	0.0125	39.061	0.173	16.089
22	10	15	500	1.0	0.0037	48.636	0.184	15.467
23	10	15	1500	1.5	0.0098	41.175	0.189	15.761
24	10	15	2500	2.0	0.0182	34.798	0.191	15.368
25	10	20	500	1.5	0.0049	46.196	0.195	15.288
26	10	20	1500	2.0	0.0132	38.588	0.217	14.931
27	10	20	2500	1.0	0.0245	32.216	0.231	13.657

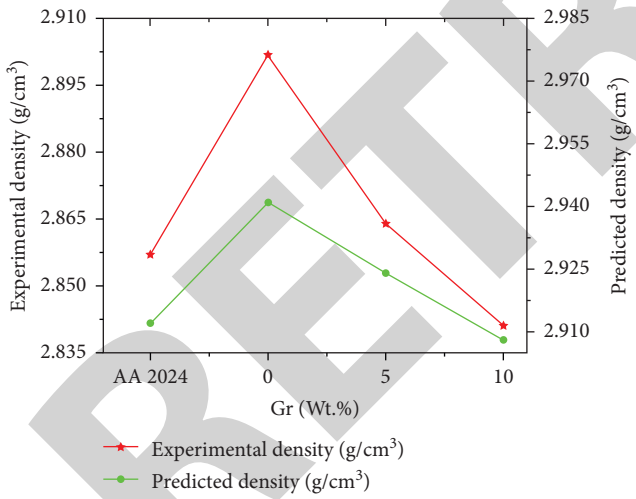

Figure 2: Experimental and predicted density of fabricated nanocomposites.

nanocomposites with wear and coefficient of friction used in this study are tabulated, respectively. Table 6 shows that the sliding distance ($p = 72.09$) significantly impacts wear loss. In addition to this, the graphite content ($p = 9.53$), load ($p = 13.95$), and sliding velocity ($p = 0.49$) of all these parameters have a minor impact on the wear loss. In contrast, interactions did not show any significant effect.

Similarly, from Table 7, it shows that the graphite content ($p = 11.12$ percent) significantly impacts the coefficient of friction. The contribution coefficient of friction is less significant for the load ($p = 60.23$ percent), sliding distance ($p = 3.25$ percent), and sliding speed ($p = 8.63$ percent). The interaction AxC ($p = 2.53$ percent) has a relatively minor effect on the friction coefficient, but the remaining interactions have no effect. As a result, sliding distance is the most important testing parameter for reducing wear loss. However, the most important factor influencing the coefficient of friction has been discovered to be graphite reinforcement.

3.4. Impact of Testing Parameters over Wear Loss. The influence of various tests and their respective interactions are plotted on wear loss of the nanocomposites, and their significant effects are plotted for the S/N ratio graph, as shown in Figure 4. It is predicted that there will be no significant effect if the constraint line of the main effect plot is significantly closer to the horizontal line. Furthermore, the parameters that will have the most significant impact on the cable are heavily skewed. The figure shows that the sliding distance is the most critical parameter, whereas other parameters such as graphite (Gr), applied load, and sliding speed had less impact on the wear loss. From all these statements, we can say that when the contact time increases, the sliding distance also increases, resulting in a massive area of contact, which affects the formation of wear debris [30]. Wear loss appears to rise as the applied stress and sliding distance increase, indicating that more materials are being

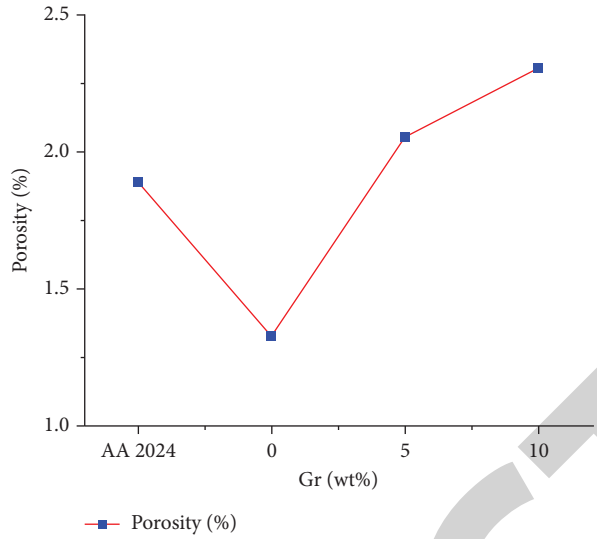

Figure 3: Attained porosity results for fabricated nanocomposites.

removed from the surface. Furthermore, when the sliding speed was increased, wear loss gradually decreased, resulting in the formation of a rich graphite layer on the fractured surface. This phenomenon reduces the wear effect by creating more contact areas. The composite with 10% graphite content reported superior wear resistance at higher loads compared to other conditions.

3.5. Impact of Testing Parameters on the Coefficient of Friction. The consequences of testing parameters and the interaction plot on the coefficient of friction and their respective effect plot for the S/N ratio are shown in Figures 5 and 6. Because parameter A has achieved the highest inclination, the grain reinforcement has a similar effect on the composite coefficient of friction, while sliding speed, distance, and load have just attained a lesser impact when compared to others. On the other hand, the coefficient of friction is nearly invariant with the sliding distance for entirely fabricated composites. The main reason behind this is that the proportion of graphite in all the samples is considered more stable. The coefficient of friction in all the composites increases significantly when the weight percentage of graphite increases. This phenomenon is observed until the graphite weight percent reaches 10% [31]. This is because the aluminum matrix contains graphite, which functions as a superb lubricant by spreading over the entire topography and producing a thick layer of lubricating coating on the surface, which eventually reduces friction by limiting contact on the sliding surface. When the percentage of graphite on the surface is greater than 10%, the friction increases due to the oxide layer's fracture within the surface, weakening the fractured surfaces. The cohesion of sliding surfaces generates abrasion because it causes interaction between the specimen and the counter, which eventually increases the coefficient of friction [32].

3.6. Linear Regression Models. General linear regressions were used to determine the interactions between the components (A) graphite weight percentage, (B) load, (C) sliding distance, (D) sliding speed, and the measured constraints. The following regression equations were eventually applied to wear and the coefficient of friction in the following equations:

$$1.\ \text{Wearloss}\,(\text{g}) = -0.0008704 + 0.000136389A + 2.77778e-7B + 2.05e-6C + 0.00134444D - 1.23333e-5A*B - 3.283333e-7A*C + 5.75e-7B*C, \quad (2)$$

$$2.\ \text{Co}-\text{efficientoffriction} = 0.0899537 - 0.00066666A + 0.003B + 1.73889e - 5\text{C}0.0016666D - 0.00016A*B + 1.33333e-7A*C - 4.66667e-7B*C. \quad (3)$$

The wear loss and coefficient of friction qualities of the manufactured samples were further evaluated within the range of variables before testing, replacing the computed values of the relevant variables with those from equations (2) and (3). Figure 7 shows a standard probability plot of the residuals used to check the model's validity as described by equations (2) and (3). The actual impacts are detected using the standard probability plot, whereas the points are very close to the average probability line in the central limit theorem. The researcher [22] reveals that the model

Table 6: ANOVA for wear loss, using adjusted SS for tests.

Source	Degrees of freedom (DOF)	Sum of squares (SS)	Adjusted sum of squares (ASS)	Adjusted mean of squares (AMS)	*F*-value	*P* value	Percentage of contribution
A	2	0.0001320	0.0001320	0.0000660	117.85	0.002	9.53
B	2	0.0002888	0.0002888	0.0001444	261.45	0.001	13.95
C	2	0.0014915	0.0014915	0.0007458	1387.12	0.000	72.09
D	2	0.0000103	0.0000103	0.0000052	9.65	0.013	0.49
A*B	4	0.0000060	0.0000060	0.0000015	1.81	0.125	0.29
A*C	4	0.0000334	0.0000334	0.0000083	0.45	0.003	1.64
B*C	4	0.0001037	0.0001037	0.0000259	0.75	0.025	1.86
Error	6	0.0000032	0.0000032	0.0000005			0.15
Total	26	0.0020689					100

$S = 0.000731817$ R-Sq = 99.84% R-Sq (adj) = 99.33%.

Table 7: ANOVA for the friction coefficient, using adjusted SS for tests.

Source	Degrees of freedom (DOF)	Sum of squares (SS)	Adjusted sum of squares (ASS)	Adjusted mean of squares (AMS)	*F*-value	*P* value	Percentage of contribution
A	2	0.0037443	0.0037443	0.0018721	7.95	0.001	11.12
B	2	0.0012574	0.0012574	0.0006287	36.41	0.002	60.23
C	2	0.0022005	0.0022005	0.0011003	0.55	0.000	3.25
D	2	0.0000130	0.0000130	0.0000065	4.56	0.813	8.63
A*B	4	0.0004846	0.0004846	0.0001211	2.01	0.064	6.98
A*C	4	0.0001015	0.0001015	0.0000254	0.84	0.547	2.53
B*C	4	0.0001650	0.0001650	0.0000413	1.37	0.349	4.03
Error	6	0.0001813	0.0001813	0.0000302			3.23
Total	26	0.0081476					100

$S = 0.00549747$ R-Sq = 97.77% R-Sq (adj) = 90.36%.

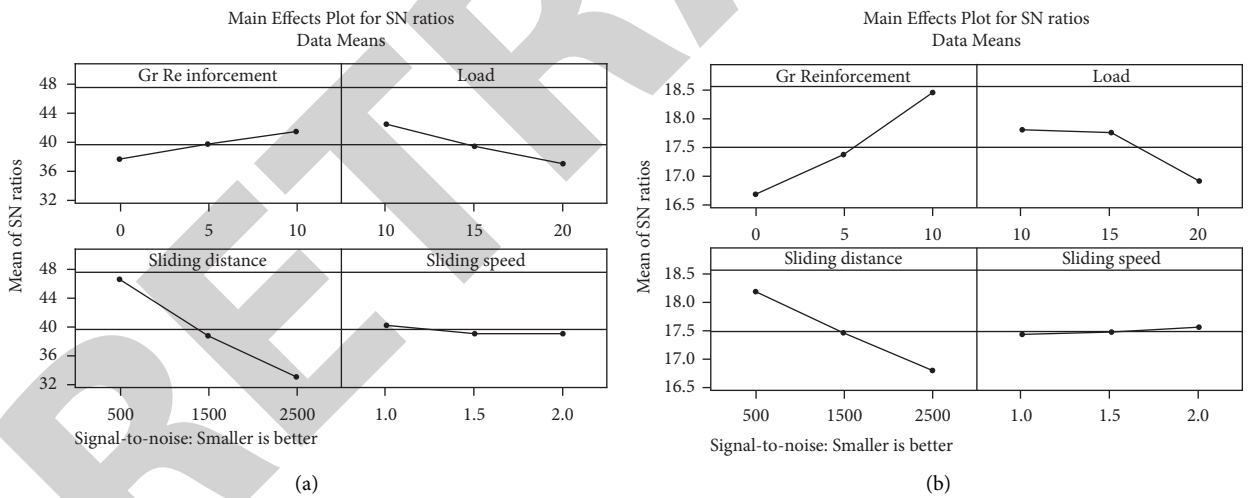

Figure 4: Main effects plot. (a) Wear loss of aluminum with a mixture of SiC and Gr hybrid nanocomposites. (b) Coefficient of friction with a blend of SiC and Gr hybrid nanocomposites.

developed for estimating both friction and wear loss of aluminum hybrid composites is represented in (2) and (3).

3.7. Examining and Assessing the Outcome of the Experiments Using the Taguchi Approach. Generally, in the Taguchi approach, we use the S/N ratio as a critical and significant component for interpreting experimental data. According to this Taguchi approach technique, the signal-to-noise ratio must have the highest value as the study determines optimal testing circumstances. The S/N ratio response tables for the coefficient of friction and wear loss characteristics are represented in Table 8. The response table gives the results of all the metric averages mentioned above at each factor level. Also, this table provides all the ranks of the impacts based on the delta statistics, which compares the degree of effects to which they are closely related [33]. The delta statistics equal each factor's highest average minus the lowest standard. Based on the results, the highest delta value earns rank one, whereas the second-highest delta value receives rank two. The evaluated coefficient of friction and wear resistance values were

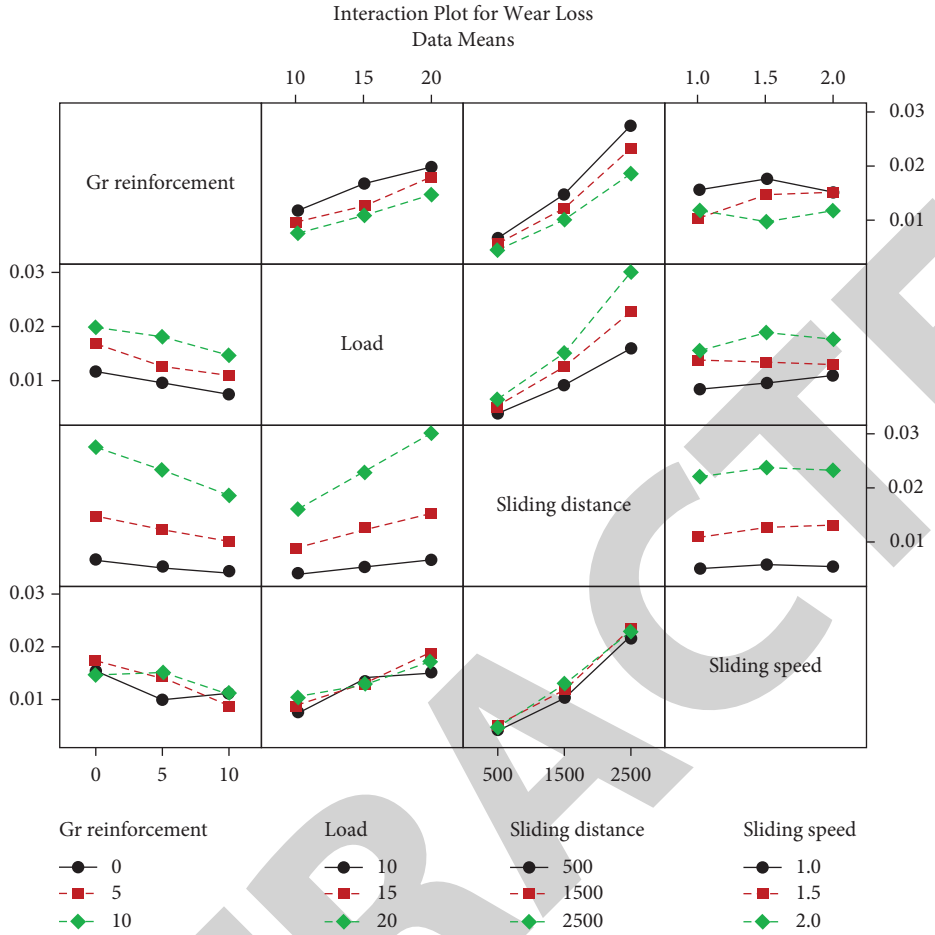

Figure 5: Interaction plots for wear loss.

10 wt. % graphite reinforcement with 10 N applied load with 500 m sliding distance and 1 m/s sliding velocity.

3.8. Confirmation Experiment. Taguchi proposes to be a confirmation test to compare the results with the investigational data. The results are confirmed based on the results drawn from the study by executing a confirmation test. After identifying the optimum and suitable conditions, a confirmation test was carried out, utilizing an amalgamation of the most satisfactory levels and comparing the results with the expected results. The wear loss in Table 9 is compared with the actual wear loss observed when ideal testing conditions are used. Both estimates are in good agreement. When perfect testing conditions are used, the S/N ratio increases by 8 dB and 4.7876 dB. It implies that the model utilized in this research can be adopted and can effectively predict the behavior of wear and coefficient of friction.

3.9. Analysis of the Fractured Surface of Counter Disc Topography. Analyzing the damaged topography of the counter disc, one can reveal the wear mechanisms that have occurred. Figure 8 represents the optical micrographs of the fractured disc surface against the composite pins. While sliding against this counterpart pin, they are irregular, uneven, and with deep grooves. A small degree of graphitic film layer may be seen in worn topography. The very thick layer of the graphite film may be seen. It implies that only minor plastic deformation occurs throughout the sliding phase. The aluminum matrix, the graphite-containing samples, produces a solid lubrication effect and improves hardness, minimizing wear loss as sliding distance increases [33].

3.10. Analysis of Worn Surfaces of Pin Using SEM. The main wear mechanisms responsible for wear loss during dry sliding tests of nanocomposites have been identified using SEM morphology investigations. The wear morphology of the AA2024 alloy's worn surface, as shown in Figure 9(a), clearly shows the presence of deep permanent grooves parallel to the sliding direction, as well as microcracks and certain damaged regions. This could be the cause of the AA2024 alloy's increased wear loss. It is also worth noting that there are not many microcracks. On the surface of the AA 2024–5 wt. percent SiC nanocomposite, oxide layers were discovered (Figure 9(b)). The presence of parallel and continuous scratches on the worn surface suggests that abrasive wear is the primary wear mechanism at work. This is due to the hard particles from the counter surface or

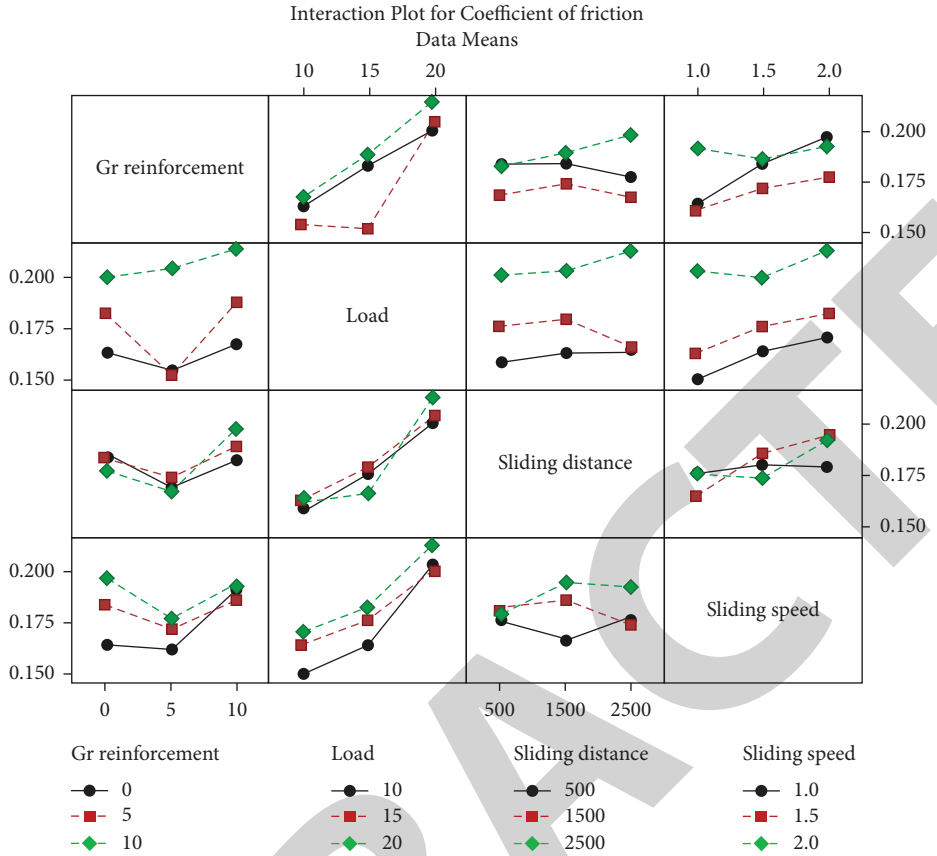

Figure 6: Interaction plots for the coefficient of friction (μ).

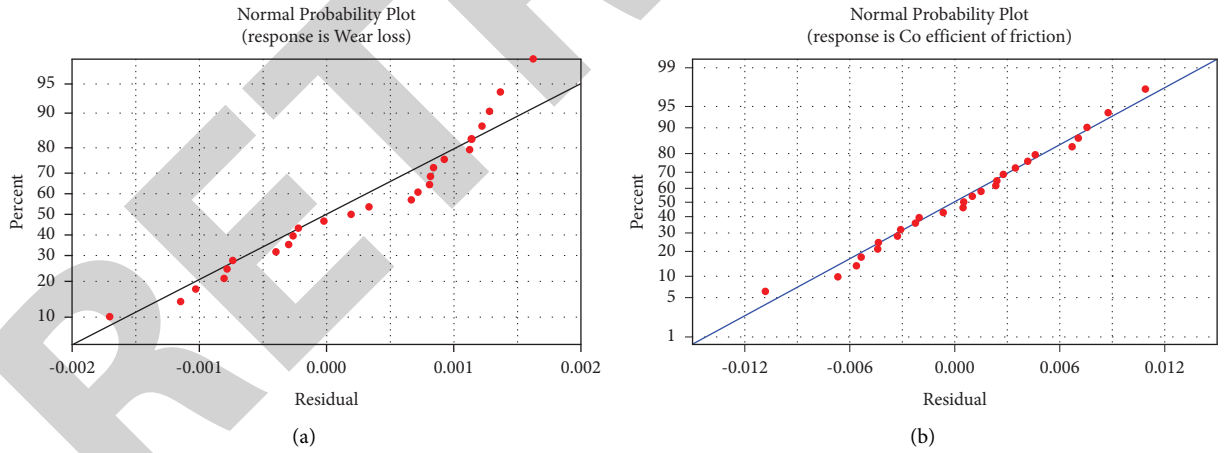

Figure 7: Standard probability plot. (a) Wear loss. (b) Coefficient of friction.

material in between the contact surfaces penetrating into the softer matrix during sliding, which contributes significantly to wear. Furthermore, the inclusion of hard SiC particles toughens the aluminum matrix, resulting in less wear. The presence of hard SiC particles in the matrix prevents the slider from cutting into the composite surface, minimizing delamination. In comparison to the pure matrix alloy and AA2024/5 wt percent SiC and smooth mechanically mixed layer, the worn morphology of hybrid nanocomposites AA2024/5 wt. percent SiC/5 wt. percent Gr and AA2024/5 wt. percent SiC/10 wt. percent Gr (Figures 9(c) and 9(d)) revealed the presence of finer grooves parallel to the sliding direction and severe plastic deformation at the edges of the grooves (MML).

The presence of graphite in the composites causes the creation of MML (tribolayer) between the sliding surfaces, giving the surface a smooth appearance. The wear morphology of the AA 2024/5 wt. percent SiC/5 wt. percent Gr

Table 8: Response table for S/N ratios: smaller is better.

Levels	Response to wear				Response to the coefficient of friction			
	A	B	C	D	A	B	C	D
1	38.71	41.46	46.77	40.34	16.68	17.89	18.30	17.50
2	39.64	39.38	38.88	39.23	17.41	17.82	17.52	17.53
3	41.51	37.03	33.22	39.30	18.56	16.94	16.83	17.62
Delta	3.80	5.43	13.55	1.11	1.86	0.95	1.46	0.13
Rank	3	2	1	4	1	3	2	4

nanocomposite is shown in Figure 9(c). Due to hand, is coated with a rather smooth MML coating, and the

Table 9: Evaluation of best outcomes of confirmation tests.

Levels	Combination of parameters A2B3C3D2	Prediction A3B1C1D1	Investigation of experimentations
Wear (g)	0.02877	0.00096	0.0015
S/N ratio (dB)	29.7326	52.1907	52.6524
Improvement of S/N ratio: 22.9198			
	A1B3C3D3	A3B1C1D1	
Coefficient of friction (μ)	0.1687	0.1044	0.1152
SN ratio (dB)	15.3819	19.6292	20.1695
Improvement of S/N ratio: 4.7876			

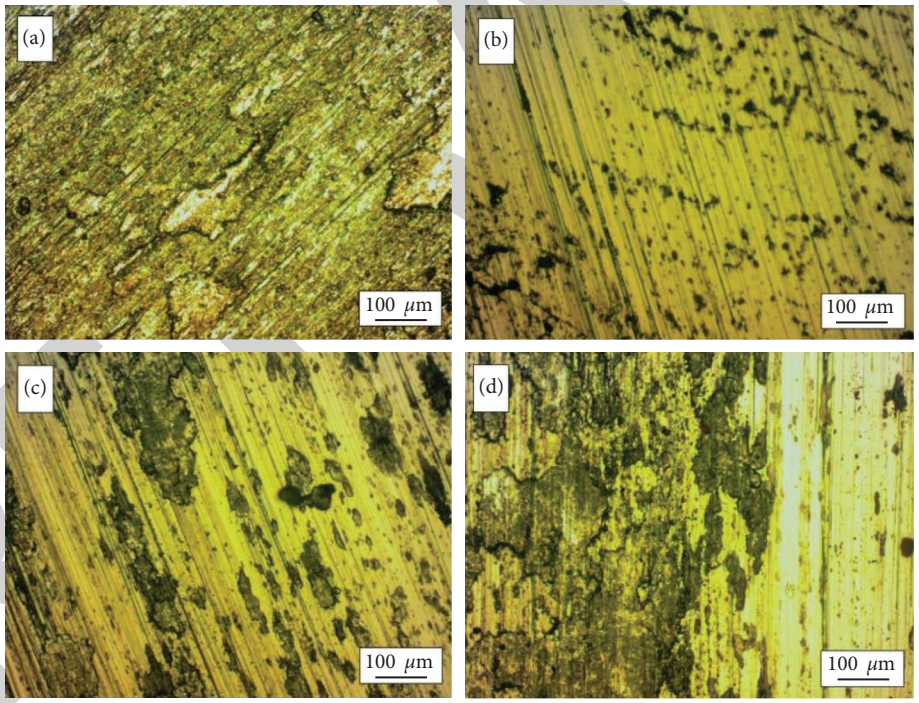

Figure 8: Optical micrographs of fractured topography of disc mated with (a) AA 2024 (b) AA 2024/5% SiC (c) AA2024/5% SiC/5% Gr (d) AA2024/5% SiC/10% Gr nanocomposite with an applied load of 15 N and at a constant speed of 1.5 m/s.

microploughing and smearing, the composite's surface is characterized by fine grooves. Furthermore, due to plastic deformation and the low fracture toughness of the graphite included in the composite, some tear edges are prone to detachment. The worn surface of the AA 2024-5 wt. percent SiC-10 wt. percent Gr composite with various wear parameters is shown in Figure 9(d). The surface morphology of AA 2024-5 wt. percent SiC-10 wt. percent Gr, on the other grooves are finer than the worn surfaces of the other nanocomposites.

The wear behavior of nanocomposites is influenced by the graphite-enriched mechanically mixed layer that forms immediately beneath the contacting surface. This MML prevents the pin from making direct contact with the counter face. As a result, abrasive wear is significantly reduced in the AA 2024–5 wt. percent SiC–10 wt. percent Gr

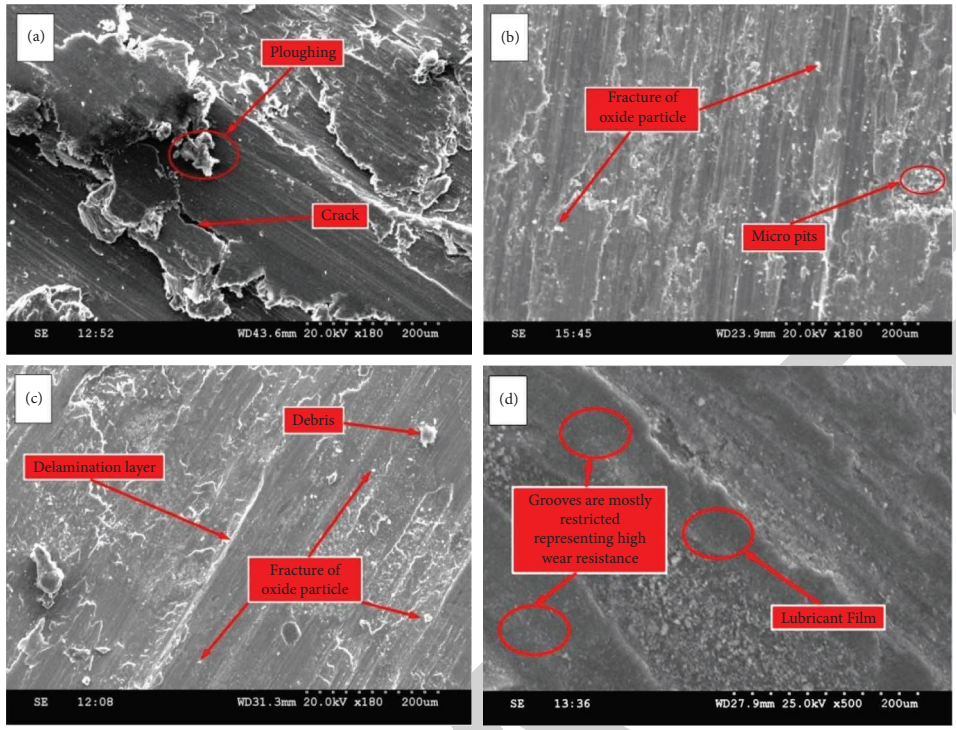

Figure 9: SEM morphologies of the worn surface of (a) AA 2024 (b) AA 2024–5 wt. % SiC (c) AA 2024–5 wt. % SiC–5 wt. % Gr (d) AA 2024–5 wt. % SiC–10 wt. % Gr composite at an applied load of 20 N and a constant speed of 2 m/s.

nanocomposites. Furthermore, delamination and oxidative wear are the most common mechanisms for material loss during sliding.

4. Conclusions

This current investigation is mainly carried out to explain the experimental methodology and utilization of optimization techniques such as the Taguchi approach to examine the various parameters which affect the wear behavior of hybrid metal matrix composites. Based on the experimental results, the following conclusions were made:

(1) Taguchi's approach of using an orthogonal array and ANOVA were adopted to evaluate the experimental results. ANOVA is used to assess the degree of the best testing parameters for wear behavior.

(2) According to the design technique ANOVA, A3B1C1D1 is considered the best combination of parameters (lowest level of load, sliding distance, speed, and highest level of graphite reinforcement). The factor of graphite nanofillers has the highest contribution to controlling friction. The characteristic of sliding distance has the maximum influence on controlling the wear behavior of hybrid nanocomposites.

(3) The wear loss and coefficient of friction polynomial models match the experimental values according to the ANOVA results. This demonstrates that the sliding distance (72.09 percent), sliding speed (0.49 percent), the load applied (13.95 percent), and graphite weight percentage in the sample (6.38 percent) are the most significant parameters impacting the sliding wear of the fabricated composites within the selected range of experiments. (Based on their contribution percentages).

(4) Analysis of Variance also reveals that the elements that most influence the friction behavior of composites within the chosen range of trials are the applied load (15.43%), sliding distance (27.00%), sliding speed (0.16%), graphite content in the composite (45.95%), and the load (7.73%) (based on their contribution percentages).

(5) Adding graphite to the aluminum alloy matrix as a subordinate reinforcement improves the material's wear resistance while lowering the porosity and density of hybrid nanocomposites. Friction coefficients and wear resistance were excellent in composites containing 10% graphite.

(6) At a 95% confidence level, there was an excellent match between anticipated and actual wear resistance. Furthermore, studies were confirmed to ensure that the best testing parameters were used.

Data Availability

The data used to support the findings of this study are included within the article. Further data or information is available from the corresponding author upon request.

Conflicts of Interest

The authors declare that there are no conflicts of interest regarding the publication of this paper.

Acknowledgments

The authors are thankful to the Vellore Institute of Technology, Chennai, for providing technical support in completing this research work. The authors appreciate the support from Wollo University, Ethiopia, for the research and preparation of this manuscript.

References

[1] P. Ravindran, K. Manisekar, P. Narayanasamy, N. Selvakumar, and R. Narayanasamy, "Application of factorial techniques to study the wear of Al hybrid composites with graphite addition," *Materials & Design*, vol. 39, pp. 42–54, 2012.

[2] S. Suresha and B. K. Sridhara, "Wear characteristics of hybrid aluminium matrix composites reinforced with graphite and silicon carbide particulates," *Composites Science and Technology*, vol. 70, no. 11, pp. 1652–1659, 2010.

[3] S. Suresha and B. K. Sridhara, "Effect of addition of graphite particulates on the wear behaviour in aluminium-silicon carbide-graphite composites," *Materials & Design*, vol. 31, no. 4, pp. 1804–1812, 2010.

[4] P. P. Ikubanni, M. Oki, A. A. Adeleke et al., "Materials today: proceedings Tribological and physical properties of hybrid reinforced aluminium matrix composites," *Materials Today Proceedings*, vol. 46, pp. 5909–5913, 2021.

[5] N. Mahaviradhan and S. Sivaganesan, "Materials today: proceedings Tribological analysis of hybrid aluminum matrix composites for high temperature applications," *Materials Today Proceedings*, vol. 39, 2020.

[6] P. Paulraj and R. Harichandran, "The tribological behavior of hybrid aluminum alloy nanocomposites at high temperature: role of nanoparticles," *Journal of Materials Research and Technology*, vol. 9, no. 5, pp. 11517–11530, 2020.

[7] V. V. Monikandan, P. K. Rajendrakumar, and M. A. Joseph, "High temperature tribological behaviors of aluminum matrix composites reinforced with solid lubricant particles," *Transactions of Nonferrous Metals Society of China*, vol. 30, no. 5, pp. 1195–1210, 2020.

[8] S. Mahdavi and F. Akhlaghi, "Effect of SiC content on the processing, compaction behavior, and properties of Al6061/SiC/Gr hybrid composites," *Journal of Materials Science*, vol. 46, no. 5, pp. 1502–1511, 2011.

[9] S. Basavarajappa, G. Chandramohan, and J. P. Davim, "Some studies on drilling of hybrid metal matrix composites based on Taguchi techniques," *Journal of Materials Processing Technology*, vol. 196, no. 1-3, pp. 332–338, 2008.

[10] P. Ravindran, K. Manisekar, S. Vinoth Kumar, and P. Rathika, "Investigation of microstructure and mechanical properties of aluminum hybrid nano-composites with the additions of solid lubricant," *Materials & Design*, vol. 51, pp. 448–456, 2013.

[11] Y. Q. Wang, A. M. Afsar, J. H. Jang, K. S. Han, and J. I. Song, "Room temperature dry and lubricant wear behaviors of Al2O3f/SiCp/Al hybrid metal matrix composites," *Wear*, vol. 268, no. 7-8, pp. 863–870, 2010.

[12] B. Hekner, J. Myalski, N. Valle, A. Botor-Probierz, M. Sopicka-Lizer, and J. Wieczorek, "Friction and wear behavior of Al-SiC(n) hybrid composites with carbon addition," *Composites Part B: Engineering*, vol. 108, pp. 291–300, 2017.

[13] S. Basavarajappa, G. Chandramohan, K. Mukund, M. Ashwin, and M. Prabu, "Dry sliding wear behavior of Al 2219/SiCp-Gr hybrid metal matrix composites," *Journal of Materials Engineering and Performance*, vol. 15, no. 6, pp. 668–674, 2006.

[14] B. N. Sarada, P. S. Murthy, and G. Ugrasen, "Hardness and wear characteristics of hybrid aluminium metal matrix composites produced by stir casting technique," *Materials Today Proceedings*, vol. 2, no. 4-5, pp. 2878–2885, 2015.

[15] A. Gupta, Renu, S. Ranjan Kumar, C. Goswami, and T. Singh, "Wear behavior of Al6061 nanocomposite reinforced with nanozirconia," *Materials Today Proceedings*, vol. 48, pp. 1112–1116, 2022.

[16] P. P. Ikubanni, M. Oki, A. A. Adeleke, and O. O. Agboola, "Optimization of the tribological properties of hybrid reinforced aluminium matrix composites using Taguchi and Grey's relational analysis," *Scientific African*, vol. 12, Article ID e00839, 2021.

[17] S. Basavarajappa, G. Chandramohan, and J. Paulo Davim, "Application of Taguchi techniques to study dry sliding wear behaviour of metal matrix composites," *Materials & Design*, vol. 28, no. 4, pp. 1393–1398, 2007.

[18] W. H. Yang and Y. S. Tarng, "Design optimization of cutting parameters for turning operations based on the Taguchi method," *Journal of Materials Processing Technology*, vol. 84, no. 1-3, pp. 122–129, 1998.

[19] R. Thiyagarajan and M. Senthil kumar, "A review on closed cell metal matrix syntactic foams: a green initiative towards eco-sustainability," *Materials and Manufacturing Processes*, vol. 36, no. 12, pp. 1333–1351, 2021.

[20] A. Haiter Lenin, S. C. Vettivel, T. Raja, L. Belay, and S. C. E. Singh, "A statistical prediction on wear and friction behavior of ZrC nano particles reinforced with Al–Si composites using full factorial design," *Surfaces and Interfaces*, vol. 10, pp. 149–161, 2018.

[21] I. Jenish, A. Felix Sahayaraj, M. Appadurai et al., "Fabrication and experimental analysis of treated snake grass fiber reinforced with polyester composite," *Advances in Materials Science and Engineering*, pp. 2021–13, 2021.

[22] S. S. Wulff, *A First Course in Design and Analysis of Experiments*, Taylor, vol. 57, Francis, Newyork, NY, USA, 2003.

[23] V. K. Selvaraj, J. Subramanian, M. Gupta, M. Gayen, and L. B. Mailan Chinnapandi, "An experimental investigation on acoustical properties of organic PU foam reinforced with nanoparticles fabricated by hydrothermal reduction technique to emerging applications," *Journal of the Institution of Engineers*, vol. 101, no. 2, pp. 271–284, 2020.

[24] J. Subramanian, S. Vinoth Kumar, G. Venkatachalam, M. Gupta, and R. Singh, "An investigation of EMI shielding effectiveness of organic polyurethane composite reinforced with MWCNT-CuO-bamboo charcoal nanoparticles," *Journal of Electronic Materials*, vol. 50, no. 3, pp. 1282–1291, 2021.

[25] S. Vinoth Kumar, J. Subramanian, A. Giridharan, M. Gupta, A. Adhikari, and M. Gayen, "Processing and characterization of organic PU foam reinforced with nano particles," *Materials Today Proceedings*, vol. 46, pp. 1077–1084, 2021.

[26] E. B. Dean and R. Unal, "Taguchi approach to design optimization for quality and cost: an overview," *Annu Conf Int Soc Parametr Anal*, vol. 1–10, 1991.

[27] K. Yamaguchi, N. Takakura, and S. Imatani, "Materials processing technology," *Advanced Materials Research*, vol. 418–420, pp. 1–6, 2012.

[28] J. Sklar, *Minitab Manual*, Pearson publishers, Boston, MA, USA, 2013.
[29] J. P. Davim, "An experimental study of the tribological behaviour of the brass/steel pair," *Journal of Materials Processing Technology*, vol. 100, no. 1-3, pp. 273–277, 2000.
[30] L. Krishnamurthy, B. K. Sridhara, and D. A. Budan, "Comparative study on the machinability aspects of aluminium silicon carbide and aluminium graphite composites," *Materials and Manufacturing Processes*, vol. 22, no. 7-8, pp. 903–908, 2007.
[31] J. Leng, G. Wu, Q. Zhou, Z. Dou, and X. L. Huang, "Mechanical properties of SiC/Gr/Al composites fabricated by squeeze casting technology," *Scripta Materialia*, vol. 59, no. 6, pp. 619–622, 2008.
[32] Y. Sahin, "The prediction of wear resistance model for the metal matrix composites," *Wear*, vol. 258, no. 11-12, pp. 1717–1722, 2005.
[33] K. Rajkumar and S. Aravindan, "Tribological performance of microwave sintered copperTiCgraphite hybrid composites," *Tribology International*, vol. 44, no. 4, pp. 347–358, 2011.